

**Magnetite decorated graphite nanoplatelets as cost effective CO<sub>2</sub> adsorbent†**

Ashish Kumar Mishra and Sundara Ramaprabhu\*

Received 7th March 2011, Accepted 15th March 2011

DOI: 10.1039/c1jm10996k

Investigation of cost effective CO<sub>2</sub> adsorbent has been a long demanding task in the present scenario of global warming. The present work investigates the high pressure carbon dioxide capture capacity of low cost magnetite decorated functionalized graphite nanoplatelets novel nanocomposite. Graphite nanoplatelets were prepared by acid intercalation followed by thermal exfoliation. Functionalization of graphite nanoplatelets was done by treatment in acidic medium. Magnetite nanoparticles were decorated onto functionalized graphite nanoplatelets surface by a chemical method. Magnetite decorated functionalized graphite nanoplatelets nanocomposite was characterized by electron microscopy, X-ray powder diffraction pattern, surface area analysis, Raman spectroscopy and FTIR spectroscopy techniques. The carbon dioxide capture capacity was measured using high pressure Sieverts apparatus. Adsorption capacity was calculated using the gas equation and incorporating van der Waals corrections at three different temperatures (25, 50 and 100 °C). A large enhancement in carbon dioxide uptake capacity of 55%, 80%, and 90% at near 11.5 bar pressure for 100 °C, 50 °C and 25 °C, respectively, was achieved by decorating magnetite nanoparticles onto functionalized graphite nanoplatelet surface.

**Introduction**

Industrialization and globalization are responsible for the increasing level of green house gases in the environment. It has been a long demanding task to counteract the greater level of green house gases to render a cleaner environment. Carbon dioxide (CO<sub>2</sub>) is considered a major anthropogenic contribution to climate change. As a result, the current scientific research community is focusing on the investigation of different materials and techniques, which can capture large amounts of CO<sub>2</sub>. Geological sequestration and storage, mineral storage, absorbing solvents (amine base liquids), ionic liquid absorbents and solid adsorbents are used to reduce the amount of CO<sub>2</sub> in the environment.<sup>1–3</sup>

Adsorption is considered one of the most promising methods for commercial applications because of the low energy requirement, cost advantage and ease of applicability over a relatively wide range of temperatures and pressures. However, the success of this technique depends on the development of low cost adsorbents with high CO<sub>2</sub> adsorption capacity.<sup>4</sup> Previously, pressure swing adsorption (PSA) using solid sorbents has gained interest.<sup>5,6</sup> Activated carbons (ACs) and zeolite-based molecular sieves have shown much promise for achieving high adsorption

capacities.<sup>7–9</sup> One dimensional carbon based nanostructures like single-walled and multi-walled carbon nanotubes can provide a good alternative for this purpose due to their large surface area and high porosity but have some limitations due to their cost factor.<sup>10</sup> Reduction of CO<sub>2</sub> in zero valent iron and use of metal oxide as heterogeneous catalyst for CO<sub>2</sub> have been also investigated.<sup>11,12</sup> Spectroscopy studies of CO<sub>2</sub> adsorption on hydroxylated metal oxide surfaces, including iron oxide and oxide-supported metal catalysts have been reported.<sup>13,14</sup> These studies encourage the possible use of metal oxide based nanocomposites as CO<sub>2</sub> sorbents. Metal oxide nanoparticles tend to agglomerate and hence possibly result in lower CO<sub>2</sub> sorption capacity. Recently, we have demonstrated the high CO<sub>2</sub> uptake capacity for Fe<sub>3</sub>O<sub>4</sub>-MWNTs by utilizing the chemical interaction of magnetite nanoparticles (Fe<sub>3</sub>O<sub>4</sub>) along with the porous nature of the nanocomposite.<sup>15</sup> High cost of MWNTs encourages the search of low cost carbon nanomaterials as substrates for magnetite nanoparticles to achieve high CO<sub>2</sub> uptake capacity.

In the present work, magnetite (Fe<sub>3</sub>O<sub>4</sub>) nanoparticles were decorated onto functionalized graphite nanoplatelets (*f*-GNP) by a simple and cost effective chemical route to avoid the agglomeration of magnetite nanoparticles. This magnetite decorated functionalized graphite nanoplatelet (Fe<sub>3</sub>O<sub>4</sub>-*f*-GNP) nanocomposite shows physicochemical adsorption of CO<sub>2</sub>. Capture capacity of nanocomposite for CO<sub>2</sub> was calculated using gas equation including van der Waals corrections. Physicochemical adsorption of Fe<sub>3</sub>O<sub>4</sub>-*f*-GNP nanocomposite for CO<sub>2</sub> was confirmed using FTIR spectroscopy. Desorption of CO<sub>2</sub> was performed at 150 °C under vacuum (10<sup>-9</sup> bar) to regain the active

Alternative Energy and Nanotechnology Laboratory (AENL), Nano Functional Materials Technology Centre (NFMTTC), Department of Physics, Indian Institute of Technology Madras, Chennai, 600036, India. E-mail: ramp@iitm.ac.in

† Electronic supplementary information (ESI) available. See DOI: 10.1039/c1jm10996k

sites of sample for further use. Additionally, the room temperature isotherm was treated with the Dubinin–Radushkevitch (D. R.) equation to study the adsorption behavior (details given in supplementary section-1.5).<sup>†</sup> This nanocomposite can be used as a CO<sub>2</sub> adsorbent at high pressures, especially for the storage of discharged CO<sub>2</sub> from thermal power plants, steel and cement industries after compression.

## Results and discussion

### Morphological and structural analysis

The morphological studies of the prepared nanocomposite were carried out by electron microscopy techniques. SEM and TEM photographs of nanocomposite clearly suggest the almost uniform decoration of magnetite nanoparticles over the surface of *f*-GNP (Fig. 1a,b). The particle size of magnetite ranges from 5–8 nm. Energy Dispersive X-ray (EDX) analysis confirms the presence of iron, oxygen and carbon elements in this nanocomposite (Fig. 1c).

XRD pattern in Fig. 2 indicates the crystal nature of magnetic nanocomposite. XRD pattern of *f*-GNP exhibits a single carbon peak at  $2\theta$  with a value of  $26.7^\circ$  which corresponds to the graphitic layered structure. XRD pattern of Fe<sub>3</sub>O<sub>4</sub>-*f*-GNP nanocomposite exhibits the peak of magnetite at  $2\theta$  values of  $21.3^\circ$ ,  $30.5^\circ$ ,  $36.4^\circ$ ,  $43.5^\circ$ ,  $53.8^\circ$ ,  $57.7^\circ$  and  $62^\circ$  along with graphitic carbon peak at  $26.7^\circ$ . These peaks correspond to the face centered cubic structure of magnetite nanoparticles. Thus XRD pattern of nanocomposite suggests the formation of two phases, one of cubic magnetite nanoparticles and the other of graphite structure of GNP. Peaks corresponding to magnetite nanoparticles were found to be broad and less intense, which may be attributed to the small crystalline size of magnetite nanoparticles or additional presence of some amorphous magnetite nanoparticles.<sup>15,16</sup> In addition, X-ray photoelectron spectroscopy and surface area studies were performed for

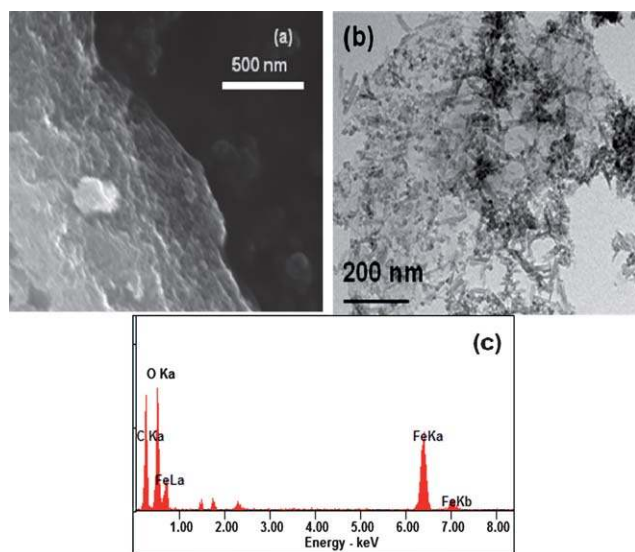


Fig. 1 SEM (a), TEM (b) images and EDX (c) analysis of Fe<sub>3</sub>O<sub>4</sub>-*f*-GNP nanocomposite.

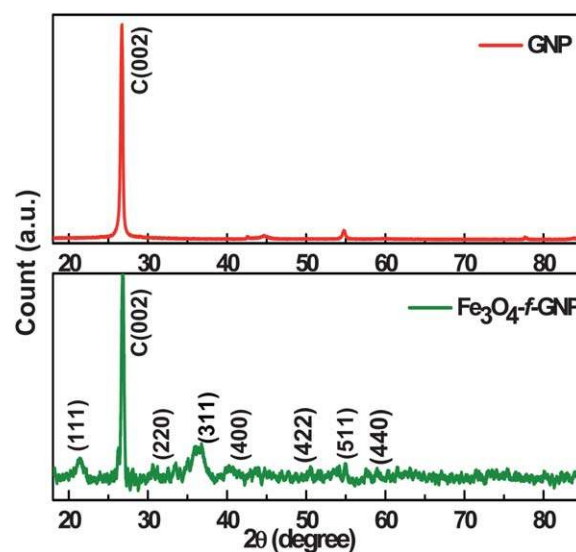


Fig. 2 X-ray diffraction pattern for GNP and Fe<sub>3</sub>O<sub>4</sub>-*f*-GNP nanocomposite.

nanocomposite. Details have been given in supplementary sections-1.2 and 1.3.<sup>†</sup>

### Adsorption isotherm studies

High pressure adsorption studies were performed using Sieverts apparatus and capture capacity was calculated using gas equation with van der Waals corrections.<sup>15</sup> Capture of CO<sub>2</sub> in Fe<sub>3</sub>O<sub>4</sub>-*f*-GNP nanocomposite was studied at three different temperatures (25, 50 and 100 °C) and at high pressures (3–12 bar) and was compared with CO<sub>2</sub> capture capacity of GNP.<sup>17</sup> Amount of CO<sub>2</sub> adsorbed in mole was measured by the following equations:

$$\Delta n_{\text{adsorbed}} = n_i - (n' + n'') \quad (1)$$

where  $n_i$  is the number of moles of CO<sub>2</sub> in the initial volume ( $V_i$ ) at the known initial pressure ( $P_i$ ) and  $n'$  is the number of moles in  $V_i$  at equilibrium pressure ( $P_{\text{eq}}$ ) and  $n''$  is the number of moles in cell volume ( $V_c$ ) at equilibrium pressure ( $P_{\text{eq}}$ ). The number of moles ( $n_i$ ), ( $n'$ ) and ( $n''$ ) can be calculated by using the following equations:

$$abn_i^3 + aV_i n_i^2 + (RT + P_i b)V_i^2 n_i - P_i V_i^3 = 0 \quad (2)$$

$$abn'^3 + aV_i n'^2 + (RT + P_{\text{eq}} b)V_i^2 n' - P_i V_i^3 = 0 \quad (3)$$

$$abn''^3 + aV_c n''^2 + (RT + P_{\text{eq}} b)V_c^2 n'' - P_{\text{eq}} V_c^3 = 0 \quad (4)$$

where ( $T$ ) is the cell temperature, ( $R$ ) is the universal gas constant, ( $a$ ) and ( $b$ ) are the van der Waals coefficient for CO<sub>2</sub> gas.

Fig. 3 shows the adsorption behavior of GNP and Fe<sub>3</sub>O<sub>4</sub>-*f*-GNP nanocomposite at three different temperatures. Maximum adsorption capacity of  $8.5 \text{ mmol g}^{-1}$  was found for Fe<sub>3</sub>O<sub>4</sub>-*f*-GNP nanocomposite and  $4.5 \text{ mmol g}^{-1}$  for GNP, at 11.5 bar and room temperature. At 11.5 bar and 50 °C maximum adsorption capacity was 7.4 and  $4.1 \text{ mmol g}^{-1}$  for nanocomposite and GNP

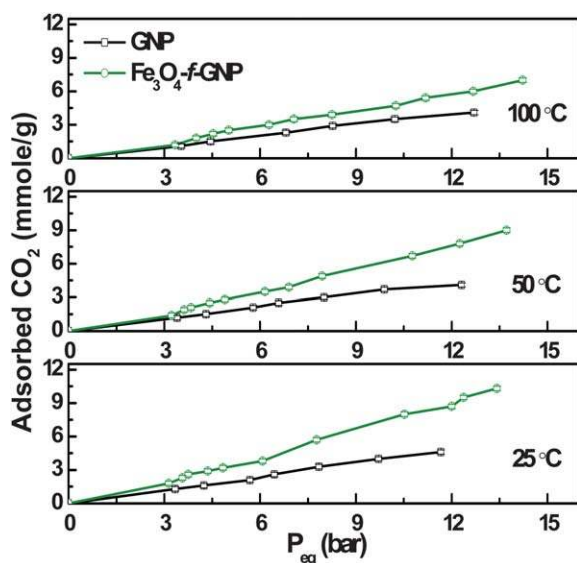


Fig. 3 Adsorption isotherms at different temperatures for GNP and Fe<sub>3</sub>O<sub>4</sub>-f-GNP nanocomposite.

respectively. At 11.5 bar and 100 °C maximum adsorption capacity was 5.6 and 3.7 mmol g<sup>-1</sup> for nanocomposite and GNP respectively. Thus, around 55% of enhancement in CO<sub>2</sub> capture capacity was achieved by decorating GNP with Fe<sub>3</sub>O<sub>4</sub> nanoparticles at 100 °C, while around 80% and 90% enhancements were obtained at 50 °C and 25 °C, respectively.

Higher CO<sub>2</sub> capture capacity of nanocomposite compared to GNP may be attributed to the additional chemical interaction of CO<sub>2</sub> molecules with magnetite nanoparticles along with physical adsorption of CO<sub>2</sub> molecules in nanocomposite. Isotherms show that at each temperature the CO<sub>2</sub> capture capacity of nanocomposite increases with increase in equilibrium pressure, which may be attributed to the possible multilayer adsorption of gas in Fe<sub>3</sub>O<sub>4</sub>-f-GNP nanocomposite along with better chemical interaction of CO<sub>2</sub> molecules with magnetite nanoparticles.<sup>15</sup> In fact, Baltrusaitis *et al.* have demonstrated the increasing intensity of carbonate and bicarbonate peaks with increase of CO<sub>2</sub> pressure for iron oxide nanoparticles.<sup>13</sup> This suggests the physicochemical adsorption of CO<sub>2</sub> in Fe<sub>3</sub>O<sub>4</sub>-f-GNP nanocomposite. Functionalization of GNP helps in better dispersion of magnetite nanoparticles and avoids the agglomeration of nanoparticles, which helps in effective utilization of magnetite nanoparticles for chemisorptions of CO<sub>2</sub>.

#### Fourier transform infrared spectroscopy analysis

FTIR study was performed to confirm the possible physicochemical adsorption of CO<sub>2</sub> in Fe<sub>3</sub>O<sub>4</sub>-f-GNP nanocomposite. Fig. 4 shows the FTIR spectrum of pristine Fe<sub>3</sub>O<sub>4</sub>-f-GNP nanocomposite and CO<sub>2</sub> adsorbed Fe<sub>3</sub>O<sub>4</sub>-f-GNP nanocomposite. FTIR study of pristine nanocomposite confirms the presence of >C=C (1634 cm<sup>-1</sup>), >C=O (1041, 1124 cm<sup>-1</sup>), -CH<sub>2</sub> (2854, 2926 cm<sup>-1</sup>), bending of =CH- (1384 cm<sup>-1</sup>) and -OH (3410 cm<sup>-1</sup>) functional groups on the surface of nanocomposite.<sup>18</sup> Along with these functional groups, bands occur at 632, 751 and 885 cm<sup>-1</sup>, which may correspond to the vibrational

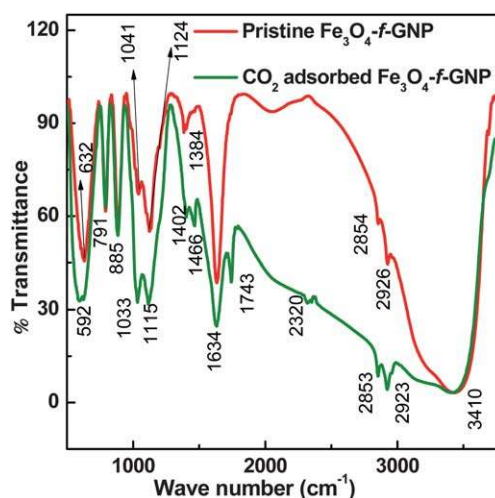


Fig. 4 FTIR spectra of pristine and CO<sub>2</sub> adsorbed Fe<sub>3</sub>O<sub>4</sub>-f-GNP nanocomposite.

modes of Fe–O bonds of Fe<sub>3</sub>O<sub>4</sub> nanoparticles and Fe–C bonds at the surface of f-GNP. Three different peaks of iron–oxygen interaction may arise due to the presence of some amorphous Fe<sub>3</sub>O<sub>4</sub> along with crystalline nanoparticles.<sup>13,16</sup>

In the case of CO<sub>2</sub> adsorbed Fe<sub>3</sub>O<sub>4</sub>-f-GNP nanocomposite, small shift was observed in all peaks. In addition, some additional peaks were noticed which may be attributed to the asymmetric stretching of adsorbed molecular CO<sub>2</sub> (2320 cm<sup>-1</sup>),<sup>19</sup> (O–C–O) symmetric vibrational mode of bicarbonates (1402 cm<sup>-1</sup>) and (C–O) symmetric vibrational mode of carbonates (1033 cm<sup>-1</sup>).<sup>13,14</sup> Some amount of bicarbonates and carbonates may be due to the strong interaction of CO<sub>2</sub> with the hydroxyl groups attached to the Fe<sub>3</sub>O<sub>4</sub> nanoparticles of nanocomposite. Peaks at 1466 and 1743 cm<sup>-1</sup> in CO<sub>2</sub> adsorbed nanocomposite may be attributed to the formation of ionic and covalent carbonates as suggested by Colthup.<sup>20</sup> Thus FTIR study confirms the chemical interaction of CO<sub>2</sub> molecules with magnetite nanoparticles along with physical adsorption of CO<sub>2</sub> in nanocomposite and hence confirms the physicochemical adsorption behavior of nanocomposite for CO<sub>2</sub>. Additionally, the physicochemical adsorption behavior of nanocomposite for CO<sub>2</sub> capture was studied with Raman spectrum study. Detail description has been given in supplementary section-1.4.†

#### Temperature dependence of CO<sub>2</sub> capture capacity

Fig. 5 shows the variation of CO<sub>2</sub> capture capacity for Fe<sub>3</sub>O<sub>4</sub>-f-GNP nanocomposite with temperature. This suggests that with increase in temperature the adsorption capacity of nanocomposite decreases. This may be attributed to the high kinetic energy of CO<sub>2</sub> gas molecules at higher temperatures, which results in higher desorption rate and less interaction of CO<sub>2</sub> with magnetite nanoparticles. At lower temperatures, due to the lower kinetic energy of CO<sub>2</sub> molecules, better interaction of CO<sub>2</sub> with nanocomposite is possible. This helps in multilayer adsorption of CO<sub>2</sub> gas as well as helps in formation of iron carbonates and bicarbonates.

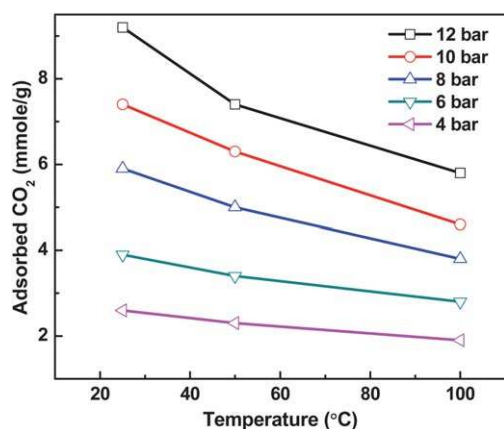


Fig. 5 Temperature dependence of adsorption capacity of Fe<sub>3</sub>O<sub>4</sub>-f-GNP nanocomposite.

### Comparison of CO<sub>2</sub> adsorption capacity with other solid sorbents

Zhang *et al.* have reported around 20% enhancement in CO<sub>2</sub> uptake by modifying the activated carbon with nitrogen at room temperature.<sup>21</sup> High pressure CO<sub>2</sub> adsorption study on different metal organic frameworks by Millward and Yaghi exhibits CO<sub>2</sub> adsorption capacity ranging from 2–8 mmol g<sup>-1</sup> at nearly 11 bar pressure and room temperature.<sup>22</sup> The present study shows a little higher CO<sub>2</sub> capture capacity at same pressure. Ease of preparation and low production cost give an edge to Fe<sub>3</sub>O<sub>4</sub>-f-GNP nanocomposite over these metal organic frameworks as CO<sub>2</sub> adsorbent. Cavenati *et al.* have reported around 5 mmol g<sup>-1</sup> of CO<sub>2</sub> adsorption in 13X zeolite at 16 bar pressure and room temperature.<sup>23</sup> The present work shows almost 70% (8.5 mmol g<sup>-1</sup>) higher CO<sub>2</sub> adsorption capacity compared to 13X zeolite even at lower pressure (11.5 bar). Low cost, easy preparation technique and higher CO<sub>2</sub> uptake capacity of Fe<sub>3</sub>O<sub>4</sub>-f-GNP nanocomposite, compared to existing adsorbents like ACs and zeolites, make it more suitable for commercial use. In addition, CO<sub>2</sub> adsorption capacities of ACs and zeolites is limited to room temperature and drastically decreases at higher temperatures, while Fe<sub>3</sub>O<sub>4</sub>-f-GNP shows high adsorption capacity up to 100 °C. This may be attributed to the fact that ACs and Zeolites includes only physical adsorption, while the present nanocomposite comprises of physical and chemical adsorption of CO<sub>2</sub>.

## Experimental section

### Synthesis of Fe<sub>3</sub>O<sub>4</sub>-f-GNP

Graphite was vigorously stirred with conc. HNO<sub>3</sub> and conc. H<sub>2</sub>SO<sub>4</sub> in 1 : 3 ratios for three days. Vigorous stirring of graphite under strong acidic medium may cause the formation of acid intercalated graphite. This intercalated graphite was further exfoliated thermally at 1000 °C. This thermal shock may lead to the destacking of the graphite plates and hence formation of GNP.<sup>17,24</sup> This GNP was further treated with conc. HNO<sub>3</sub> for 2h, which introduces hydrophilic functional groups (–COOH, –C=O, and –OH) at the surface of GNP.<sup>17</sup> Availability of functional groups was confirmed with FTIR study, details have been given in supplementary section-1.1.† These functionalized graphite

nanoplatelets (f-GNP) were further washed several times with water to achieve pH = 7 followed by drying. Functional groups at the surface of GNP provide anchoring sites for the uniform decoration of metal oxide nanoparticles over the surface of f-GNP.

Decoration of magnetite nanoparticles over the f-GNP surface was done by a chemical technique. Functionalized GNP was suspended in de-ionised water by ultrasonication method. Functional groups at the surface of f-GNP make GNP hydrophilic in nature, resulting in better dispersion of f-GNP in water. FeCl<sub>3</sub>·6H<sub>2</sub>O and FeSO<sub>4</sub>·7H<sub>2</sub>O (Across Organics) were dissolved in de-ionised water in the stoichiometric ratio of 3 : 2. This solution was heated up to 90 °C. Ammonia solution (NH<sub>4</sub>OH-25%) and f-GNP dispersed solution, in the volumetric ratio of 1 : 5, were added to the above solution. This mixture solution was stirred at 90 °C for 30 min and then cooled to room temperature. The black precipitate was collected by filtration and washed to neutral with water followed by drying. The obtained black precipitate was Fe<sub>3</sub>O<sub>4</sub>-f-GNP nanocomposite.<sup>15,25</sup>

### Characterization techniques

Fe<sub>3</sub>O<sub>4</sub>-f-GNP nanocomposite was characterized by FEI QUANTA 3D scanning electron microscope (SEM) and Philips JEOL CM12 transmission electron microscope (TEM). X-ray powder diffraction analysis was performed by X'Pert Pro PANalytical X-ray diffractometer. Surface area measurement was performed using Micromeritics ASAP 2020 surface area analyzer. Raman analysis was performed by using HORIBA JOBIN YVON HR800UV Confocal Raman spectrometer, while FTIR study was performed by using PERKIN ELMER Spectrum One FT-IR spectrometer. X-ray photoelectron spectroscopy (XPS) analysis was performed by using Omicron nanotechnology X-ray photoelectron spectrometer.

### Adsorption and desorption

Adsorption studies were carried out using high pressure Sieverts apparatus. Experimental setup consists of stainless tubes, tees, elbow joints and needle valves procured from NOVA, Switzerland and they can withstand up to 1000 bar pressure. Schematic of the experimental setup is given elsewhere.<sup>14</sup> Pressure reduction was observed using pressure transducers (pressure range 0–50 bar), procured from Burster, Germany. Numbers of cycles were performed to recheck the adsorption capacity and the values were found to be almost consistent.

After each cycle of adsorption, desorption of gas was performed under vacuum (10<sup>-9</sup> bar) at 150 °C for two hours. Physically adsorbed CO<sub>2</sub> can be removed at high temperatures in vacuum, while formed carbonates and bicarbonates are unstable with the lowering of CO<sub>2</sub> gas pressure as reported by Baltrusaitis *et al.*<sup>13</sup> This helps in regaining the active sites of nanocomposite for further capture of CO<sub>2</sub>. Desorbed sample was again used for adsorption study and adsorption capacity was found to be almost repeatable suggesting the availability of active sites after desorption for CO<sub>2</sub> capture.

## Conclusion

The present work shows a large enhancement for CO<sub>2</sub> physico-chemical adsorption capacity by decorating the magnetite (Fe<sub>3</sub>O<sub>4</sub>) nanoparticles over the surface of *f*-GNP at 25, 50 and 100 °C. At higher temperature and low pressure, enhancement may be attributed mainly to the chemical interaction of CO<sub>2</sub> molecules with magnetite nanoparticles, while at low temperature and high pressure it may be associated with additional multilayer adsorption of gas along with chemical interaction. The CO<sub>2</sub> capture capacity of nanocomposite is higher than widely used adsorbents like zeolites, activated carbon especially at higher temperatures. Cost effective preparation process of Fe<sub>3</sub>O<sub>4</sub>-*f*-GNP nanocomposite and sustainability of CO<sub>2</sub> adsorption capacity even at 100 °C compared to zeolites and activated carbon, makes this nanocomposite a suitable CO<sub>2</sub> adsorbent for industrial use, especially for the storage of discharged CO<sub>2</sub> from thermal power plants, steel and cement industries. In addition, desorption of adsorbed CO<sub>2</sub> at moderate high temperatures (150 °C) suggests the possible utilization of desorbed CO<sub>2</sub> for food, oil and chemical industries.

## Acknowledgements

The authors acknowledge the support of Office of Alumni Affairs, IIT Madras and DST, India. One of the authors (Ashish) is thankful to DST India for providing the financial support. Authors are also thankful to National Catalytic Research Center, Department of Chemistry and SAIF, IIT Madras for helping in XPS, BET and FTIR analysis.

## References

- S. Shimada, H. Y. Li, Y. Oshima and K. Adachi, *Environ. Geol.*, 2005, **49**, 44.
- W. N. Sams, G. Bromhal, S. Jikich, T. Ertekin and D. H. Smith, *Energy Fuels*, 2005, **19**, 2287.
- J. Johnson, *Chem. Eng. News*, 2004, **82**, 36.
- M. Radosz, X. Hu, K. Krutkramelis and Y. Shen, *Ind. Eng. Chem. Res.*, 2008, **47**, 3783.
- C. W. Skarstrom, U.S. Pat., 2 944 627, 1960.
- Fuderer and E. Rudelstorfer, U.S. Pat., 3 896 849, 1976.
- S. Sircar, T. C. Golden and M. B. Rao, *Carbon*, 1996, **34**, 1.
- R. V. Siriwardane, M. Shen, E. P. Fisher and J. Poston, *Energy Fuels*, 2001, **15**, 279.
- T. D. Burchell, R. R. Judkins, M. R. Rogers and A. M. Williams, *Carbon*, 1997, **35**, 1279.
- M. Cinke, J. Li, C. W. Bauschlicher Jr., A. Ricca and M. Meyyappan, *Chem. Phys. Lett.*, 2003, **376**, 761.
- G. Guan, T. Kida, T. Ma, K. Kimura, E. Abe and A. Yoshida, *Green Chem.*, 2003, **5**, 630.
- T. Hikov, A. Rittermeier, M. B. Luedemann, C. Herrmann, M. Muhler and R. A. Fischer, *J. Mater. Chem.*, 2008, **18**, 3325.
- J. Baltrusaitis, J. H. Jensen and V. H. Grassian, *J. Phys. Chem. B*, 2006, **110**, 12005.
- M. R. Nelson and R. F. Borkman, *J. Phys. Chem. A*, 1998, **102**, 7860.
- A. K. Mishra and S. Ramaprabhu, *Energy Environ. Sci.*, 2011, **4**, 889.
- D. Shi, J. P. Cheng, F. Liu and X. B. Zhang, *J. Alloys Compd.*, 2010, **502**, 365.
- A. K. Mishra and S. Ramaprabhu, *Int. J. Chem. Eng. Appl.*, 2010, **1**, 266.
- U. J. Kim, C. A. Furtado, X. Liu, G. Chen and P. C. Eklund, *J. Am. Chem. Soc.*, 2005, **127**, 241.
- W. M. Hlaing Oo, M. D. McCluskey, A. D. Lalonde and M. G. Norton, *Appl. Phys. Lett.*, 2005, **86**, 073111.
- B. Colthup, *J. Opt. Soc. Am.*, 1950, **40**, 397.
- Z. Zhang, M. Xu, H. Wang and Z. Li, *Chem. Eng. J.*, 2010, **160**, 571.
- A. R. Millward and O. M. Yaghi, *J. Am. Chem. Soc.*, 2005, **127**, 17998.
- S. Cavenati, C. A. Grande and A. E. Rodrigues, *J. Chem. Eng. Data*, 2004, **49**, 1095.
- S. Ganguli, A. K. Roy and D. P. Anderson, *Carbon*, 2008, **46**, 806.
- J. F. Liu, Z. S. Zhao and G. B. Jiang, *Environ. Sci. Technol.*, 2008, **42**, 6949.